

MECHANICAL AND METALLURGICAL PROPERTIES OF WIDE-GAP ALUMINOTHERMIC RAIL WELDS

A. Mohassel*, A. H. Kokabi and P. Davami

* *abbas.mohassel@yahoo.com*

Received: June 2011

Accepted: October 2011

Department of materials science and engineering, Sharif University of Technology, Tehran, Iran.

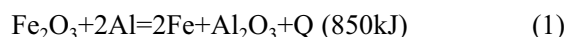
Abstract: *The wide-gap aluminothermic rail welds with root opening of 50-70 mm were produced using plain carbon steel rail and non-alloy aluminothermic charge. Mechanical properties and micro-structure of the weld metal and HAZ as well as the impact energy and the fracture toughness of the welds were investigated. The yield and tensile strength of wide-gap welds were about 98% and 95% of the base metal, respectively. Both minimum and maximum hardnesses of the joint were seen in HAZ which were related to the grain coarsening and normalizing, respectively. The mean value of wide-gap weld fracture toughness is more than narrow-gap weld. Moreover, trans-granular cleavage indicated the brittle fracture mode of the weld metal.*

Keywords: *Wide-gap weld, Aluminothermic weld, Fracture toughness, Microstructure.*

1. INTRODUCTION

Wide-gap aluminothermic rail welds have proved their abilities in decreasing the number of welds in the track and in making the repair of faulty rails more efficient. Repairing a defective rail can be performed by cutting the defect out and using two standard or narrow-gap welds and a rail plug typically 4.5 to 6 meters long. A relatively long rail plug is required to ensure that if one weld fails in service, the other will be remote enough not to be damaged by the break. The current process removes an actual defect but introduces two new probable faults. The problem can be solved using only one wide-gap weld with a width of 2-3 inches which improves the track integrity by reducing the total number of welds in the track and saves both time and money. The extended gap allows defective or broken welds to be directly repaired by a single weld. Wide-gap welds offer reduced cost, less track-occupancy time and increased safety, all by reducing the number of welds in the track. It can save money up to \$900 per defective rail according to a 1997 cost analysis performed by Transportation Technology Center, Inc [1]. Both the standard and the wide-gap welds are made via aluminothermic welding which is the world-wide preferred method for joining rails in the track. It uses heat generated from a highly exothermic reaction between fine aluminum and iron oxide powders to make a melt which then, pours into a

prepared gap between the rails to be joined. Sand moulds fit around the rail ends and hold the molten steel until it solidifies. The typical reaction in the aluminothermic welding of rails is as Eq. (1) [2]:



There are only few researches on the performance of wide-gap aluminothermic rail welds and those published in mechanical characterization of aluminothermic welds by Myers et al. [3], Schroeder and Poirier [4] and Meric et al. [5] are all in the narrow-gap weld category. None of the specimens prepared by Meric was included in both the weld metal and the HAZ of the weldment, to make proper study of the tensile behavior of the weld. Few data in some aspects of wide-gap aluminothermic rail welds including fracture toughness have been recorded in scientific literatures [6]. The present study aimed to investigate the mechanical properties of the wide-gap aluminothermic rail welds including the fracture toughness as well as the macro- and microstructure of the weld. The tensile behavior, hardness profile and microstructure of the HAZs of the welded rail were also studied.

2. EXPERIMENTAL PROCEDURES

The wide-gap aluminothermic rail welds with

Table 1. Chemical composition of the base metal (Wt.%)

| C | Mn | Si | S | P |
|-------|-------|-------|-------|-------|
| 0.534 | 0.880 | 0.240 | 0.024 | 0.016 |

Table 2. Mechanical properties of the base metal

| Yield Strength (Mpa) | Tensile Strength (Mpa) | Elongation (%) | Hardness (HB) |
|----------------------|------------------------|----------------|---------------|
| 418 | 816 | 8 | 245 |

Table 3. Components of Aluminothermic Mixture (Wt.%)

| Iron Oxide Brash | Aluminum Powder | Flake Steel Brash | Ferroalloy Pellets |
|------------------|-----------------|-------------------|--------------------|
| 64.9 | 19.64 | 9.5 | 5.96 |

root opening of 50-70 mm were produced using the UIC60-grade 700A plain carbon steel. Tables 1 and 2 show chemical composition and mechanical properties of the base metal, respectively. The hot rolled microstructure of the base metal consisting of ferrite and pearlite is shown in Fig.1. The charge components used in the current work are shown in Table 3. Self-tapping thimble which was positioned in the crucible base center was designed to allow the resultant aluminothermic steel to automatically tap into the moulds when the slag/metal separation was completed at 2040 °C [2]. Since the root gap accepted by the wide-gap aluminothermic rail welds is about three times of

the standard welds, the outlet cross section of the thimble was calculated to provide the volume flow rate which is three times that of the standard thimble. Therefore, the tapping time for wide-gap welds was the same as that for the standard welds and hence, the early solidification of the melts was prevented. The rail ends were preheated to about 850 °C by a flame torch. Tensile specimens (sub size samples according to ASTM A370) were prepared from the head sections of the weldment, across the weld metal and HAZ of the welded rails, as shown in Fig. 2. The Rockwell hardness measurements were made on specimens across the weld metal and both HAZ of the

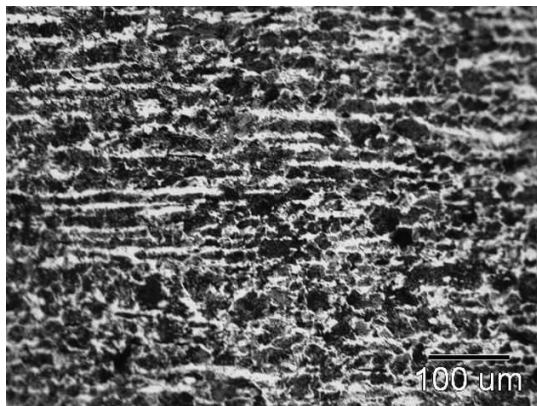


Fig. 1. Microstructure of the base metal.

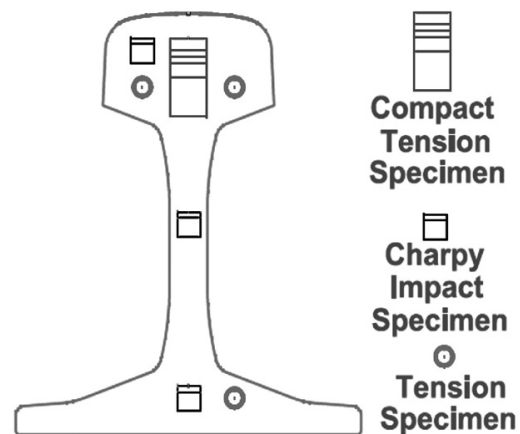


Fig. 2. The position of Tensile, Charpy Impact and Compact Tension Specimens in the Rail Welding Zone.

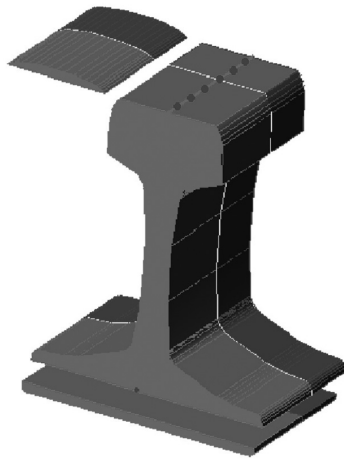


Fig. 3. The position of hardness testing in the Weld and HAZ.

weldment. Fig. 3 shows the position of hardness testing points in the welding zone and HAZ of the weldment. Charpy V-notch specimens were prepared from the head, web and the base of the weld metal according to ASTM E23-62. Impact tests were conducted only on specimens taken from the weld metal and were performed at five temperatures of 0, 20, 50, 100 and 150 °C. The resistance of aluminothermic rail weld against brittle fracture in the presence of a flaw was studied by performing fracture toughness tests on three Compact Tension (CT) samples at room temperature in accordance to ASTM E-399. The sides of the samples were polished to facilitate crack detection. A notch with root radius of 50 micron and perpendicular to the longitudinal rail direction was placed in weld metal with an a/w ratio of 0.23-0.33. All of the specimens were fatigue pre-cracked on a servo-hydraulic machine with an a/w of 0.52-0.55. The machine operated

under displacement-controlled conditions at a displacement rate of 0.5 mm.min⁻¹. Fracture surfaces and micro-structures of the tensile and impact specimens were characterized using a SEM equipped with EDS to determine the type of inclusions found in the weld metal. These specimens were etched with 2% Nital reagent.

3. RESULTS AND DISCUSSION

3. 1. Tensile Properties

Table 4 compares the tensile properties of the narrow and wide gap welds with the base metal. The tensile and yield strength of the wide gap joint were about 95% and 98% of the base metal, respectively. According to Table.4, the tensile strength of the wide gap weld was significantly higher than narrow gap weld. Therefore, it proved the capability of wide gap welds application instead of narrow gap welds.

3. 2. Hardness Properties

The hardness profile and microstructures of the HAZ and weld metal are shown in Figs. 4 and 5, respectively. As it was seen, the hardness magnitude increased to a maximum near to the boundary between the fusion zone and the HAZ, and then decreased to a second minimum close to the interface of the HAZ and the base metal. As a result of high weld metal temperature, grain coarsening (~60 μm average grain size) was occurred in the minimum hardness region of the HAZ near the base metal (Fig. 5a). Moreover, the minimum hardness was more likely due to the spheroidization of cementite platelets in the

Table 4. Tensile properties of the base metal? narrow and wide-gap welds

| Property | Base metal | Narrow-Gap Welding [5] | Wide-Gap Welding (Current Study) |
|-----------------------|------------|---------------------------|-------------------------------------|
| Yeild Strength(MPa) | 415 | 412 | 408 |
| Tensile Strength(MPa) | 816 | 722 | 774 |
| Elongation(%) | 9 | 4 | 3 |

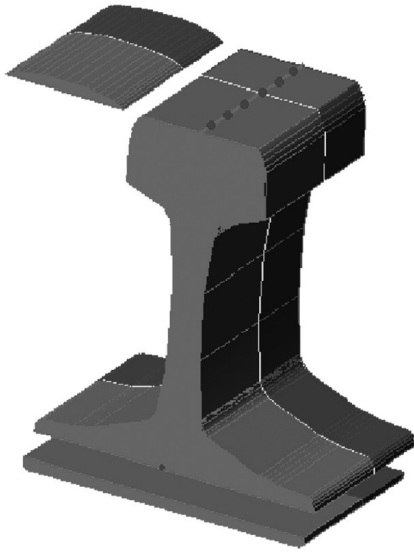


Fig. 4. Hardness variations across the joint.

pearlite colonies [7]. The hardness increase seen in the HAZ adjacent to the weld metal may be attributed to grain refining ($\sim 25 \mu\text{m}$ average grain size) due to normalizing phenomenon above the steel's critical range [7,13,14] (Fig. 5b). In all cases, both the maximum and minimum hardness were occurred in HAZ. The weld metal showed a minimum hardness at the center. It may be related to the coarse grains formed in this region because of high volume of weld metal and low cooling rate in this welding process (Fig. 6).

3. 3. Impact Properties

The impact energies at various temperatures for the sample with 60 mm root gap are shown in Fig. 7.

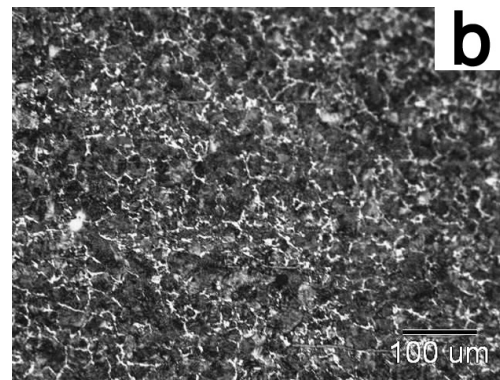
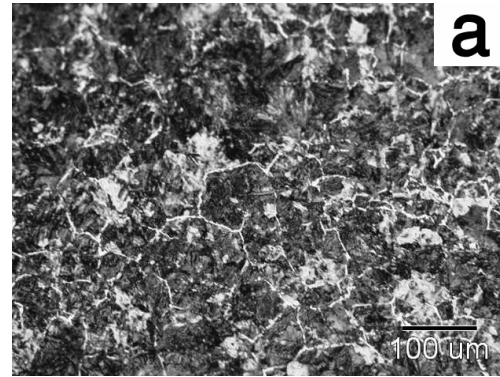


Fig. 5. The microstructure of HAZ, (a) near the base metal (50 mm distance from the weld center) and (b) near the fusion zone (30 mm distance from the weld center).

At 20 °C, the impact energy was only 4.0 J while the absorbed energy was 6.7 J and 16.2 J at 100 °C and 150 °C, respectively. It is a proof of denoting to the low impact properties as well as the high ductile-brittle transformation temperature for the wide-gap welds. The low values of the obtained impact energies indicated the brittle fracture mode of the weld metal. Fig. 8 shows the fracture surface of a

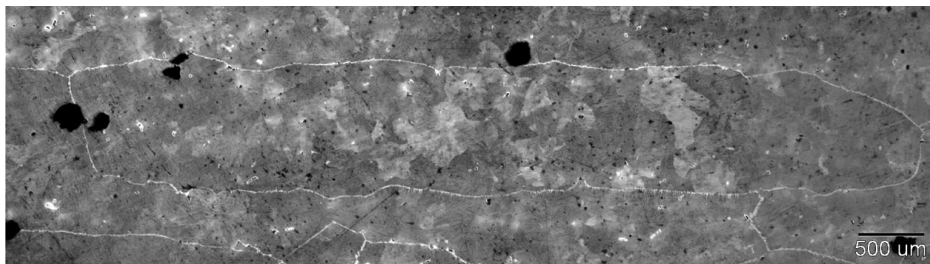


Fig. 6. The microstructure of weld metal.

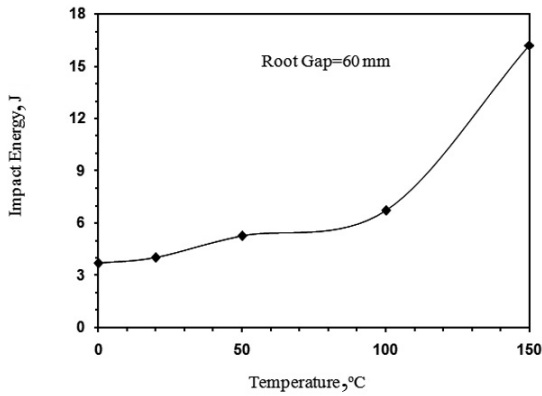


Fig. 7. Charpy impact energy of the joints vs. temperature.

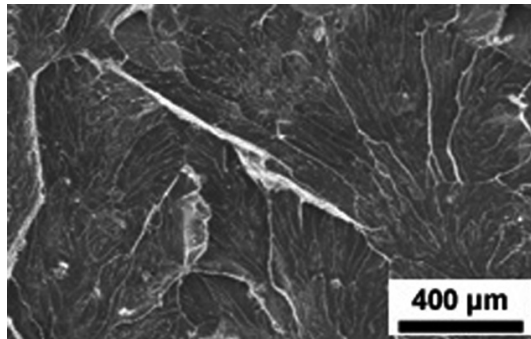


Fig. 8. Fracture surface of a Charpy impact specimen from the weld.

Charpy impact specimen indicating the transgranular cleavage and thus, the brittle mode of fracture.

3. 4. Fracture Toughness Test

The result of COD test is depicted in Fig. 9. An initial linear region precedes an obvious deviation from linearity, followed by an increase in load to a maximum value. All specimens

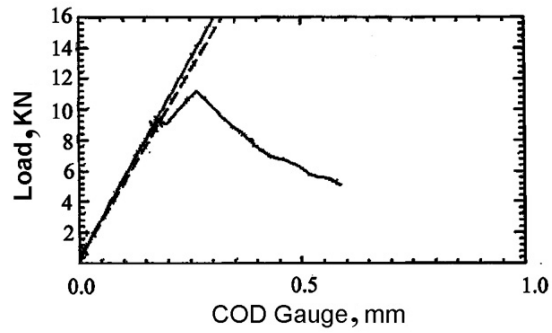


Fig. 9. Load vs. COD Plot.

exhibited non-catastrophic fracture under the substantial cracking occurrence after the maximum load. Table 5 compares the results of wide gap welds with the base metal and narrow gap welds reported in literatures, according which the fracture toughness mean value of wide and narrow gap welds was about 75% and 60% of the base metal, respectively. The mean value of wide-gap weld fracture toughness was lower than the average of those reported for carbon steel rails and higher than narrow-gap welds.

3. 5. Inclusions

Visual examination of the weld surfaces showed a few isolated nonmetallic macro-inclusions in some welds. These inclusions were 1-4 mm in size located in the web and head of the weld centerline where final segregation occurred. Fig. 10 shows the EDS results of such inclusions indicating the presence of iron oxide inclusions. Sand particles were produced as a result of washing during the pouring or due to blowing from the mould prior to welding. Macro-porosity is the other feature which was seen in small quantities in the surface of the fractured

Table 5. Results of fracture toughness test

| The base metal | Narrow-Gap Weld | Wide-Gap Weld |
|-----------------------------|-----------------------------|----------------------------------|
| 44±3(MPa m ^{1/2}) | 28.6(MPa m ^{1/2}) | 33.5± 1.5(MPa m ^{1/2}) |
| | Other researches [8-12] | current study |

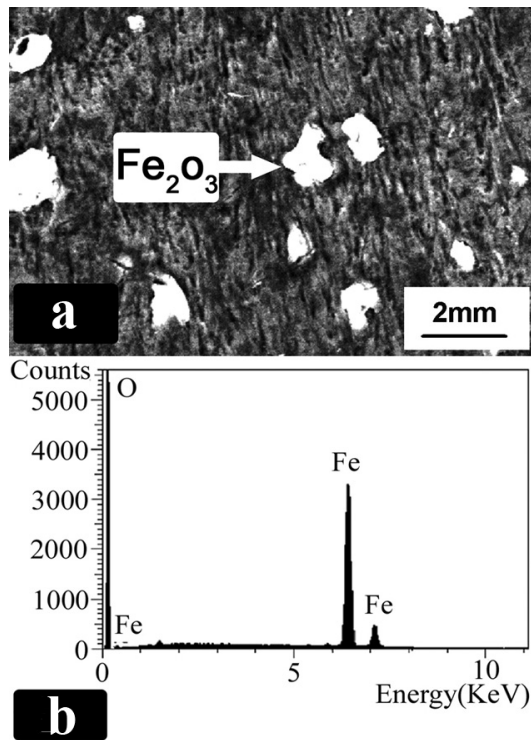


Fig. 10. a: Inclusion (unreacted iron oxide) in the fracture surface of Charpy impact specimen.
b: result of EDS analysis of inclusion found in a.

specimens. Most of them were oriented in the weld metal centerline in the direction of heat flow. This type of feature and some of the observed inclusions have also been seen in the narrow-gap aluminothermic welds [3,5]. Fig. 11 shows the macro-porosities observed in the

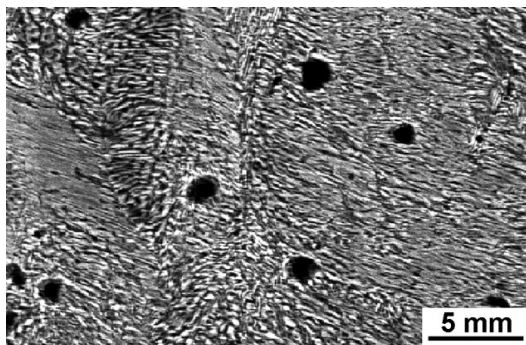


Fig. 11. Macro-Porosity in weld zone.

surface of the tensile specimen fractured in the welding zone.

4. CONCLUSIONS

1. Wide gap aluminothermic rail welding proved its capability for being used in the repair of defective rails.
2. The wide gap joint strength reached 95% of the base metal strength.
3. Grain coarsening and normalizing caused the minimum and maximum hardness of HAZ, respectively. Minimum hardness at the center of the weld may be related to the coarse grains formed in this region because of low cooling rate.
4. Trans-granular cleavage indicated the brittle fracture mode of the weld metal.
5. The mean value of wide-gap weld fracture toughness was higher than narrow-gap welds.

5. ACKNOWLEDGEMENT

The authors would like to thank the staff of Manufacturing and Production Department, IRRC, especially Mr. H. Saharkhiz, Mr. H. Yazdani and Ms. N. Jalali for their contributions throughout the study.

We wish to thank the Iran Railways Research Center (IRRC) for the financial support of this project. We also gratify Razi Metallurgy Research Center (RMRC) for its useful supports.

REFERENCES

1. Sawley, K. and Sun, J., Wide-gap Welds Offer Railroads Potential Saving. *Railw. Track and Struct.*, 1999, 4, 12.
2. Meric, C. and Engez, T., Understanding the Aluminothermic Welding Process. *Weld. J.*, 1999, 78, 33.
3. Myers, J., Geiger, G. H. and Poirier, D. R., Structure and Properties of Aluminothermic Welds in Rail. *Weld. J.*, 1982, 61, 258s.
4. Schroeder, L. C. and Poirier, D. R., The Mechanical Properties of Aluminothermic Welds in Premium Alloy Rails. *Mater. Sci. Eng A.*, 1984, 63, 1.

5. Meric, C., Atik, E. and Sahin, S., Mechanical and Metallurgical Properties of Welding Zone in Rail Welded Via Aluminothermic Process. *Sci. Technol. Weld. Joining.*, 2002, 7, 172.
6. Jian, S. and Sawley, K., Laboratory Evaluation of Wide Gap Thermite Rail Welds. *AAR Technology Digest*.1998, October (TD-98-026), 95.
7. Linnert, G. E., *Welding Metallurgy Carbon and Alloy Steels*, 4th ed. Florida, USA, 1994, pp. 878-883.
8. Orringer, O., Morris, J. M. and Steele, R. K., Applied research on Rail Fatigue and Fracture in United State. *Theor. Appl. Fract. Mech*, 1984, 1, 23.
9. Alexander, D. J. and Bernstein, I. M., Microstructural Control of Flow and Fracture in Pearlitic Steel. *TMS-AIME*, 1984, 243.
10. Igwemezi, J. O., Kennedy, S. L., Feng, X. and Cai, Z., "Defective rail fracture under dynamic, thermal and residual stresses" *Proceedings of 5th Intl. Heavy Haul Conf*, Beijing, China, 1993, 6-13.
11. Lewandowski, J. J., Mechanical behavior of in-situ composites. *TMS-AIME*, 1994, 159.
12. Lonsdale, C. P. and Lewandowski, J. J., "Fracture toughness of aluminothermic rail weld steel" *Proceedings of 39th MWSP Conf.*, Indianapolis, USA, 1998, 1083-1090.
13. Golmahalleh, O. and Zarei-Hanzaki, A., Strain Induced Austenite-to-Ferrite Transformation Behavior Of Plain Carbon Steels Through Single Pass Rolling. *Iran. J. Mater. Sci. Eng.*, 2004, 1 (1), 9.
14. Esmailian, M., The Effect of Cooling Rate and Austenite Grain Size on the Austenite to Ferrite Transformation Temperature and Different Ferrite Morphologies In Microalloyed Steels. *Iran. J. Mater. Sci. Eng.*, 2010, 7 (1), 7.